Sodium Intercalation into the $n = 2$ Ruddlesden−Popper Type Host $Y_2Ti_2O_5S_2$: Synthesis, Structure, and Properties of α-$Na_xY_2Ti_2O_5S_2$ ($0 < x \leq 1$)

Simon J. Clarke,* Sophie G. Denis, Oliver J. Rutt, Timothy L. Hill, Michael A. Hayward, Geoffrey Hyett, and Zoltán A. Gál

Inorganic Chemistry Laboratory, Department of Chemistry, University of Oxford, South Parks Road, Oxford, OX1 3QR, U.K.

Received August 18, 2003. Revised Manuscript Received October 30, 2003

Sodium intercalation into the oxide slabs of the cation-deficient $n = 2$ Ruddlesden−Popper oxysulfide $Y_2Ti_2O_5S_2$ to produce α-$Na_xY_2Ti_2O_5S_2$ ($0 < x \leq 1.0$) is reported. These materials have been probed as a function of the amount of intercalated sodium using high-resolution neutron powder diffraction. At all levels of sodium intercalation the tetragonal symmetry of the host is retained, for example: $Na_{0.35(5)}Y_2Ti_2O_5S_2$, *I*4/*mmm*, $a = 3.80171(2)$ Å, $c = 22.6270(2)$ Å, $Z = 2$; $Na_{0.84(2)}Y_2Ti_2O_5S_2$, *I*4/*mmm*, $a = 3.84429(6)$ Å, $c = 22.5440(4)$ Å, $Z = 2$ at 298 K. The sodium ion occupies a site coordinated by twelve oxide ions which corresponds to the "*A*"-site in the perovskite-like oxide slabs of the structure. At levels of sodium intercalation up to the maximum α-$Na_{1.0}Y_2Ti_2O_5S_2$ the cell volume increases approximately linearly with *x* as electrons enter bands which are antibonding with respect to the Ti−O framework. The effects on the structural details of electrostatic repulsion between the yttrium and intercalated sodium ions is discussed, and these materials are compared with the analogous lithium intercalates. Magnetic susceptibility and electrical resistivity measurements are consistent with delocalization of the intercalated electrons especially for large *x*. The insertion of lithium into α-$Na_{0.5}Y_2Ti_2O_5S_2$ and of magnesium into $Y_2Ti_2O_5S_2$ are also reported.

Introduction

Intercalation is important in the modification of materials properties.[1,2] Reductive topotactic insertion of alkali metals into transition metal oxides[3] and sulfides[4] has been explored extensively in the context of producing electrochromic devices and for battery technology.[5,6,7] We have recently reported[8] two products which result from the intercalation of alkali metals into materials which show features of both perovskite-related oxides with vacant "*A*" sites, such as WO_3, and layered sulfides. The oxysulfides $Ln_2Ti_2O_5S_2$ (Ln = Pr − Er, Y)[9,10] have structures similar to those of the $n = 2$ Ruddlesden−Popper (R−P) phases[11] which have the general stoichiometry $AX(AMX_3)_n$ and comprise perovskite blocks *n* layers of octahedra thick, separated by *AX* "rock salt" layers; the oxysulfides have a 12-coordinate vacant site in the oxide slabs. Lithium (introduced either using the vapor, *n*-BuLi, or Li in liquid ammonia)[12] inserts into 4-coordinate sites, which are the windows separating the vacant 12-coordinate sites, to give a limiting composition of $Li_2Ln_2Ti_2O_5S_2$. Sodium, when introduced as the vapor at between 400 and 600 °C, inserts into the 12-coordinate vacancy to give a limiting stoichiometry of $Na_{1.0}Ln_2Ti_2O_5S_2$.[8] However, when inserted using sodium naphthalide in THF,[8] sodium is unable to enter the 12-coordinate site via the 4-coordinate window and so enters sites tetrahedrally coordinated by sulfide in the LnS "rock salt" layers with a consequent cell expansion of 30% along the direction perpendicular to the layers in the structure. Reductive intercalation into the rock salt layers of a R−P phase was unprecedented, although it is reminiscent of the *oxidative* intercalation of fluorine into R−P phases such as the $n = 2$ R−P phase $Sr_3Ru_2O_7$.[13] The products of intercalation of sodium into the oxide layers are designated α-$Na_xLn_2Ti_2O_5S_2$ ($0 < x \leq 1$), and the metastable products of sodium intercalation into the sulfide layers are designated *β*-$NaLn_2Ti_2O_5S_2$ which are line phases. On heating at 600 °C in evacuated silica tubes, the *β*-$NaLn_2Ti_2O_5S_2$ phases transform irreversibly to the α-$NaLn_2Ti_2O_5S_2$ phases.[8] Potassium only inserts into the sulfide layers in the formation of $KY_2Ti_2O_5S_2$[14] and this entails a relative shift of adjacent oxide slabs to

* To whom correspondence should be addressed. Tel: +44 1865 272600. Fax: +44 1865 272690. E-mail: simon.clarke@chem.ox.ac.uk.

(1) Murphy, D. W. *Advances in the Synthesis and Reactivity of Solids*; A Research Annual; JAI Press: Greenwich, CT, 1991; Vol. 1, p 237.
(2) Rouxel, J.; Tournoux, M. *Solid State Ionics* **1996**, *84*, 141.
(3) Chippindale, A. M.; Dickens, P. G.; Powell, A. V. *Prog. Solid State Chem.* **1994**, *21*, 133.
(4) Eichhorn, B. W. In *Progress in Inorganic Chemistry Vol. 42*; Karlin, K. D., Ed.; Wiley: New York, 1994.
(5) Bruce, P. G. *Chem. Commun.* **1997**, 1817.
(6) Murphy, D. W.; Sunshine, S. A.; Zahurak, S. M. *NATO ASI Series B* **1987**, *172*, 173.
(7) Murphy, D. W. *NATO ASI Series E* **1985**, *101*, 181.
(8) Denis, S. G.; Clarke, S. J. *Chem. Commun.* **2001**, 2356.
(9) Goga, M.; Seshadri, R.; Ksenofontov, V.; Gütlich, P.; Tremel, W. *Chem. Commun.* **1999**, 979.
(10) Boyer, C.; Deudon, C.; Meerschaut, A. *C. R. Acad. Sci. Paris, Ser. II* **1999**, *2*, 93.
(11) Ruddlesden, S. N.; Popper, P. *Acta Crystallogr.* **1958**, *11*, 541.
(12) Hyett, G.; Rutt, O. J.; Gál, Z. A.; Hayward, M. A.; Clarke, S. J. *J. Am. Chem. Soc.* Submitted for publication.
(13) Li, R. K.; Greaves, C. *Phys. Rev. B* **2000**, *62*, 3811.

10.1021/cm034762f CCC: $25.00
Published on Web 11/27/2003

enable K^+ to occupy a site in which it is in square prismatic coordination by sulfide. The general scheme is summarized in ref 14. Most of the chemistry has been reported using the diamagnetic $Y_2Ti_2O_5S_2$ as the host. Here we describe the systematic insertion of sodium into the oxide layers of $Y_2Ti_2O_5S_2$ to form α-$Na_xY_2Ti_2O_5S_2$ ($0 < x \leq 1$) which is best accomplished by reacting together appropriate ratios of $Y_2Ti_2O_5S_2$ and β-$NaY_2Ti_2O_5S_2$ at temperatures between 500 and 600 °C. The products are compared with the range of lithium intercalates, which are reported in detail elsewhere,[12] and the products of intercalation of both sodium and lithium, and of magnesium into the oxide slabs are reported briefly.

Experimental Section

Synthesis of Sodium Intercalates. β-$NaY_2Ti_2O_5S_2$ is extremely air-sensitive, and oxidizes in a matter of seconds when exposed to air. All manipulations of solids were therefore carried out in a Glovebox Technology argon-filled recirculating drybox with a combined O_2 and H_2O content of less than 5 ppm. Orange $Y_2Ti_2O_5S_2$ was prepared on the 2−10 g scale by reacting stoichiometric quantities of Y_2O_3, TiO_2, and TiS_2 at 1100 °C in sealed silica tubes. Y_2O_3 (Aldrich 99.99%) was dried at 900 °C for 24 h in air and then removed to the drybox; TiO_2 (Aldrich 99.9+ %) was dried at 250 °C in air; and TiS_2 was prepared by reacting Ti (ALFA 99.99%, dehydrided) with S (ALFA 99.9995%) at 600 °C for 3−4 days in evacuated silica tubes. (Caution: the temperature was raised slowly from 400 to 600 °C over 24 h to avoid a build-up of sulfur pressure). The starting materials were ground and loaded into a silica tube which had been baked at 900 °C under a vacuum of 2 10^{-2} mbar for several hours to remove adsorbed moisture. This prebaking step is important to minimize contamination of the oxysulfide with $Y_2Ti_2O_7$. The tube was sealed under a vacuum of 10^{-3} mbar and the oxysulfide was obtained phase pure according to laboratory powder X-ray diffraction (PXRD) by heating at 1100 °C for 3−4 days. Sodium intercalation to produce β-$NaY_2Ti_2O_5S_2$ was carried out by reacting 2−3 g of $Y_2Ti_2O_5S_2$ with a 2-fold molar excess of sodium naphthalide in THF using Schlenk techniques. Naphthalene (Aldrich 98%) was dissolved in THF which had been dried by distillation over potassium. This solution was stirred at room temperature with a 2-fold molar excess of freshly cut sodium chips for 24 h to form 0.05 M sodium naphthalide solution. This deep green solution was added to the $Y_2Ti_2O_5S_2$ powder and the suspension was stirred for 7 days at 50 °C. The blue-black β-$NaY_2Ti_2O_5S_2$ was isolated by filtration, washed 3× with fresh, dry THF, and dried under vacuum prior to removal to the drybox. PXRD confirmed that the product was single phase β-$NaY_2Ti_2O_5S_2$.[8] Samples of α-$Na_xY_2Ti_2O_5S_2$ with $x = 0.35(5)$, 0.72(5), 0.84(2), and 0.95(2) were prepared by reacting together the appropriate amounts of β-$NaY_2Ti_2O_5S_2$ with $Y_2Ti_2O_5S_2$. The mixtures were ground thoroughly and loaded into silica tubes of 9-mm or 12-mm o.d. which had been previously flame-dried under vacuum. The tubes were sealed under a vacuum of 10^{-3} mbar and placed in a chamber furnace at temperatures between 500 and 600 °C. The synthetic details of the samples used for neutron powder diffraction investigations and property measurements are summarized in Table 1. Chemical analysis was used to confirm sodium content, as β-$NaY_2Ti_2O_5S_2$ prepared by the naphthalide route sometimes contains some NaH impurity[8] which provides an additional sodium content in the products. The structure and properties of α-$Na_{1.00(2)}Y_2Ti_2O_5S_2$ prepared by reacting $Y_2Ti_2O_5S_2$ with sodium vapor in a sealed nickel tube at 600 °C have been described previously[8] and are included here for comparison. In contrast with β-$NaY_2Ti_2O_5S_2$,[8] and the lithium intercalates,[12] the α-$Na_xY_2Ti_2O_5S_2$ intercalates are fairly resistant to aerial hydrolysis, but were also stored in the drybox.

Table 1. Summary of Synthesis of Samples α-$Na_xY_2Ti_2O_5S_2$

x in $Na_xY_2Ti_2O_5S_2$	synthetic method	T (°C)	duration (d)
0.35(5)	$Y_2Ti_2O_5S_2 + \beta$-$NaY_2Ti_2O_5S_2$	510	5
0.72(5)	$Y_2Ti_2O_5S_2 + \beta$-$NaY_2Ti_2O_5S_2$	510	5
0.84(2)	$Y_2Ti_2O_5S_2 + \beta$-$NaY_2Ti_2O_5S_2$	550	6
0.95(2)	$Y_2Ti_2O_5S_2 + \beta$-$NaY_2Ti_2O_5S_2$	550	6
1.00(2)[a]	$Y_2Ti_2O_5S_2$ + Na vapor	600	7

[a] Sample described in ref 8.

The results of systematic lithium intercalation[12] showed that reduction to Ti^{III} was possible at below room temperature using a lithium/ammonia solution at −78 °C as the reductant. Attempts to insert additional sodium into α-$Na_{0.5}Y_2Ti_2O_5S_2$ or α-$Na_{1.0}Y_2Ti_2O_5S_2$ were carried out either by grinding the compounds with a 2-fold molar excess (added Na/Ti = 1:1) of NaH and heating in sealed glass tubes at 250 °C for 2 days, or by reacting the compounds with sodium/ammonia solution (added Na/Ti = 1:1) overnight at −78 °C. Although these conditions produce β-$NaY_2Ti_2O_5S_2$ from $Y_2Ti_2O_5S_2$,[14] there was no change in lattice parameters of the α-$Na_xY_2Ti_2O_5S_2$ intercalates after reaction, and it seems impossible to intercalate substantial amounts of sodium simultaneously into the oxide and sulfide layers, presumably due to the competing changes in Ti-environment which would be required.[8] Attempts to intercalate further lithium into α-$Na_{1.0}Y_2Ti_2O_5S_2$ were similarly unsuccessful, but the reaction between α-$Na_{0.5}Y_2Ti_2O_5S_2$ and lithium/ammonia solution (Li/Ti = 1:1) overnight at −78 °C, followed by washing of the solid in dry THF to remove the $LiNH_2$ formed by decomposition of the excess metastable lithium/ammonia solution,[12] did yield a double intercalate of lithium and sodium as discussed below.

Synthesis of Magnesium Intercalates. Magnesium may be intercalated chemically into layered TiS_2 up to $Mg_{0.22}TiS_2$,[15] and electrochemically into a series of oxides such as WO_3.[16] Intercalation of Mg into $Y_2Ti_2O_5S_2$ was carried out by grinding excess MgH_2 (Aldrich 95%) (Mg/Ti = 1:1) with 2.5 g of $Y_2Ti_2O_5S_2$ and heating the mixture in a sealed silica tube at 300 °C for two periods of 2 days with intermediate regrinding. Unreacted MgH_2 was then removed by washing the sample with 0.1 M hydrochloric acid solution. Reaction of $Y_2Ti_2O_5S_2$ with excess (Mg/Ti = 5:1) 1 molar dibutylmagnesium in hexane at 50 °C resulted in decomposition to form MgH_2 with no measurable change of lattice parameters of $Y_2Ti_2O_5S_2$, consistent with the difficulty in intercalating Mg chemically into WO_3.[15] Attempts to intercalate the other alkaline earths from metal/ammonia solutions at −78 °C resulted only in decomposition of these solutions.

Chemical Analysis. Analysis for sodium, magnesium, and lithium was carried out using a Thermo Elemental Atomscan 16 ICP analyzer. The sodium and magnesium ions were leached out of the intercalates by boiling the materials in 50% nitric acid solution in silica tubes, and lithium ions were leached out by water alone.

Diffraction Measurements. Powder X-ray diffraction (PXRD) measurements to assess phase purity and determine lattice parameters were carried out using a Siemens D5000 diffractometer operating in Debye−Scherrer geometry with Cu $K\alpha_1$ radiation selected using a Ge(111) monochromator. Samples were ground with amorphous boron (1:1 mass ratio) to limit sample absorption and sealed in 1-mm diam glass capillaries. Powder neutron diffraction (PND) measurements were carried out using the diffractometer POLARIS at the ISIS Facility, Rutherford Appleton Laboratory, U.K. Samples of approximately 1−2 g mass were measured in the d-spacing range $0.5 < d < 8$ Å by means of three banks of detectors located at scattering angles 2θ of 35° (^{3}He tube detector), 90° (ZnS scintillator), and 145° (^{3}He tube detector, highest resolution

(14) Rutt, O. J.; Hill, T. L.; Gál, Z. A.; Hayward, M. A.; Clarke, S. J. *Inorg. Chem.* **2003**, ASAP Article October 25, 2003.

(15) Bruce, P. G.; Krok, F.; Nowinski, J.; Gibson, V. C.; Tavakkoli, K. J. *Mater. Chem.* **1991**, *1*, 705.

(16) Gregory, T. D.; Hoffman, R. J.; Winterton, R. C. *J. Electrochem. Soc.* **1990**, *137*, 775.

Table 2. Refinement Results from PND Data for Phases α-$Na_xY_2Ti_2O_5S_2$ and $Mg_{0.32(2)}Y_2Ti_2O_5S_2$

compound	$Na_{0.35(5)}Y_2Ti_2O_5S_2$	$Na_{0.72(5)}Y_2Ti_2O_5S_2$	$Na_{0.84(2)}Y_2Ti_2O_5S_2$	$Na_{0.95(2)}Y_2Ti_2O_5S_2$	$Mg_{0.32(2)}Y_2Ti_2O_5S_2$
instrument	POLARIS	POLARIS	POLARIS	POLARIS	POLARIS
temperature/K	298	298	298	298	298
space group	*I*4/*mmm*	*I*4/*mmm*	*I*4/*mmm*	*I*4/*mmm*	*I*4/*mmm*
a/Å	3.80171(2)	3.83652(4)	3.84429(6)	3.85185(9)	3.82308(4)
c/Å	22.6270(2)	22.4977(3)	22.5440(4)	22.5937(6)	22.6523(3)
V/Å^3	327.029(5)	331.142(9)	333.17(2)	335.22(2)	331.09(1)
variables	60	77	82	85	100
χ^2	1.375	1.527	1.896	[a]2.452	2.556
wR_p	0.0167	0.0169	0.0194	0.0231	0.0230
$R(F^2)$	0.0309	0.0340	0.0413	0.0462	0.0703

[a] Value using unsplit O1 site was 2.678; lattice parameters were unchanged within 3σ.

bank: $\Delta d/d = 5\ 10^{-3}$) for a total integrated proton current at the production target of about 600/*m* μAh, where *m* is the mass in grams of the sample. All samples for neutron diffraction measurements were contained in 6-mm or 10-mm diam thin-walled vanadium cans which were sealed in the drybox with indium gaskets. Temperatures below room temperature were achieved using an "ILL Orange" cryostat. Rietveld refinement against POLARIS data utilized all three detector banks simultaneously, and was carried out using the GSAS suite of programs.[17]

Magnetic Susceptibility Measurements. Measurements were carried out using a Quantum Design MPMS2 SQUID magnetometer in the temperature range 5−320 K and at magnetic fields of up to 5 T. A 30−100-mg portion of material was loaded into predried (100 °C) gelatine capsules. Measurements of the susceptibility were made by measuring the moment of the sample at fields of 4 and 5 T and determining the gradient of moment against field in this region. This was necessary because measurements of sample moment against field showed that the samples, which have small paramagnetic moments, invariably contained miniscule amounts of ferromagnetic impurities (probably nickel) which saturated at fields above 1 T. Corrections for core diamagnetism were carried out using standard tables.[18]

Electrical Resistivity Measurements. Measurements were carried out by cold-pressing pellets of material 5-mm in diameter and approximately 1-mm thick at 0.5 GPa and measuring the resistance using a 2-probe method in the drybox.

Results

Sodium Intercalation. The products of the reactions were all dark green ($x < 0.7$) or black ($0.7 < x < 1.0$) powders. The synthesis of the materials with $x < 0.7$ was effected by the reaction between β-$NaY_2Ti_2O_5S_2$ and $Y_2Ti_2O_5S_2$ at temperatures as low as 510 °C for 5 days, producing well-crystallized α-$Na_xY_2Ti_2O_5S_2$ phases with Bragg peaks roughly 10−20% broader than those of the starting materials. In the synthesis of the more Na-rich materials ($x > 0.7$) it was found that temperatures of 550 °C were required to produce materials with *x* up to 0.95 with Bragg peaks which were 50% broader than those of the starting materials. In the annealing of pure β-$NaY_2Ti_2O_5S_2$, temperatures of 630 °C were required to obtain α-$Na_{1.0}Y_2Ti_2O_5S_2$ far inferior in terms of crystallinity (Bragg peaks 70% broader) to that obtained by the reaction of $Y_2Ti_2O_5S_2$ with sodium vapor at 600 °C.[8] The advantage of using the solid-state reaction between β-$NaY_2Ti_2O_5S_2$ and $Y_2Ti_2O_5S_2$ over the reaction of $Y_2Ti_2O_5S_2$ with sodium vapor is that the composition can be more readily controlled − particularly at small *x*, and the amounts of decomposition products identified previously[8] ($YTiO_3$ and $NaYS_2$) can be minimized. However, the solid-state route results in less well crystallized material, particularly at $x \sim 1$, than the vapor intercalation route which produces material with Bragg peaks only about 10% broader than those of $Y_2Ti_2O_5S_2$.[8] This is presumably a consequence of a decrease in particle size and introduction of strain inherent in the deintercalation of Na from β-$NaY_2Ti_2O_5S_2$ and reinsertion to form α-$Na_{1.0}Y_2Ti_2O_5S_2$.

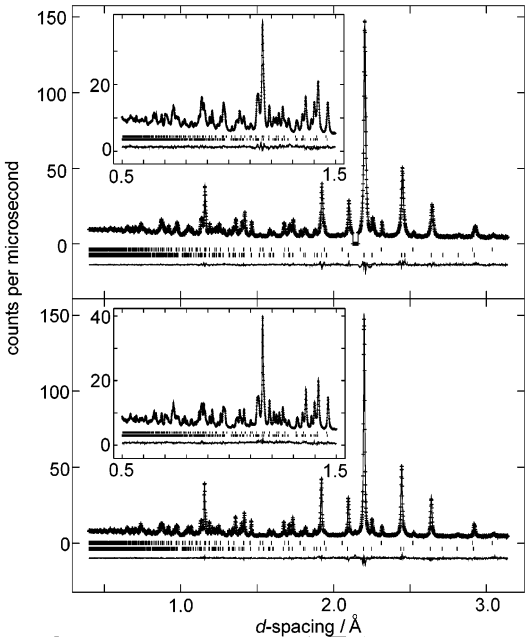

Figure 1. Results of Rietveld refinements of the structures of α-$Na_{0.72(5)}Y_2Ti_2O_5S_2$ (bottom) and α-$Na_{0.84(2)}Y_2Ti_2O_5S_2$ (top) against POLARIS data (145° detector bank). The measured (points), calculated (line), and difference (lower line) profiles are shown. Tick marks indicate allowed reflections for the $Na_xY_2Ti_2O_5S_2$ phase (lower set) and 2 mol % of a $Y_2Ti_2O_7$ impurity (upper set). A Bragg peak arising from the vanadium sample container has been excluded from the refinement for α-$Na_{0.84(2)}Y_2Ti_2O_5S_2$. The insets show magnifications of the low *d*-spacing regions.

The PXRD patterns indicated materials isostructural with α-$Na_{1.00(2)}Y_2Ti_2O_5S_2$,[8] with topotactic sodium intercalation into the oxide blocks of the $Y_2Ti_2O_5S_2$ host. This was confirmed by the analysis of PND data (Table 2), using the structure of α-$Na_{1.00(2)}Y_2Ti_2O_5S_2$[8] as a starting model with starting lattice parameters for each phase derived from PXRD measurements. Fits to the PND patterns for α-$Na_{0.72(5)}Y_2Ti_2O_5S_2$ and α-$Na_{0.84(2)}Y_2Ti_2O_5S_2$ are shown in Figure 1. The structural model obtained for α-$Na_{1.00(2)}Y_2Ti_2O_5S_2$[8] showed that the aniso-

(17) Larson,A.; von Dreele, R. B. *The General Structure Analysis System*; Los Alamos National Laboratory: Los Alamos, NM, 1985.
(18) Landolt-Bornstein New Series II/10: *Magnetic Properties of Transition Metal Compounds*, Supplement 2; Springer-Verlag: Berlin, 1979.

Table 3. Atomic Parameters for Samples α-$Na_xY_2Ti_2O_5S_2$ and $Mg_{0.32(2)}Y_2Ti_2O_5S_2$ Obtained from Refinement against PND Data

refined parameter	$Na_{0.35(5)}Y_2Ti_2O_5S_2$ ($I4/mmm$)	$Na_{0.72(5)}Y_2Ti_2O_5S_2$ ($I4/mmm$)	$Na_{0.84(2)}Y_2Ti_2O_5S_2$ ($I4/mmm$)	$Na_{0.95(2)}Y_2Ti_2O_5S_2$ ($I4/mmm$)	$Mg_{0.32(2)}Y_2Ti_2O_5S_2$ ($I4/mmm$)
			Y (0 0 *z*)		
z	0.33377(1)	0.33366(2)	0.33328(2)	0.33280(3)	0.33380(3)
100 × ($U_{iso,eq}$/Å^2)	0.58(1)	0.64(1)	0.66(1)	0.71(2)	0.84(2)
			Ti (0 0 *z*)		
z	0.08050(2)	0.08246(3)	0.08287(4)	0.08344(5)	0.08144(5)
100 × ($U_{iso,eq}$/Å^2)	0.41(2)	0.35(2)	0.33(2)	0.46(4)	1.26(3)
			O1 (0 $^1/_2$ *z*) or O1 (*x* $^1/_2$ *z*)[a]		
z	0.09912(1)	0.09869(1)	0.09841(2)	0.09778(3)	0.10032(2)
x	-	-	-	0.0523(3)	-
100 × ($U_{iso,eq}$/Å^2)	0.67(1)	0.89(1)	1.69(4)	1.21(4)	1.52(3)
			O2 (0 0 0)		
100 × ($U_{iso,eq}$/Å^2)	1.61(2)	1.69(3)	1.52(3)	1.43(5)	1.99(4)
			S (0 0 *z*)		
z	0.20441(3)	0.20463(4)	0.20442(4)	0.20492(6)	0.20583(6)
100 × ($U_{iso,eq}$/Å^2)	0.55(2)	0.65(3)	0.53(3)	0.53(5)	0.92(4)
			Na (Mg) (0 0 $^1/_2$)		
100 × ($U_{iso,eq}$/Å^2)	2.5(1)	3.0(1)	2.5(1)	2.1(1)	3.9(2)
Na (Mg) Fraction	0.349(3)	0.712(5)	0.828(5)	0.941(6)	[b]0.32

[a] Split site has 50% occupancy. [b] Not refined.

Table 4. Selected Bond Distances (in Å) and Bond Angles (in degrees) for Intercalates $Na_xY_2Ti_2O_5S_2$ and $Mg_{0.32(2)}Y_2Ti_2O_5S_2$; Numbers in Square Brackets Indicate the Number of Bonds or Angles of a Particular Type

	[a]$Y_2Ti_2O_5S_2$	$Na_{0.35(5)}Y_2Ti_2O_5S_2$	$Na_{0.72(5)}Y_2Ti_2O_5S_2$	$Na_{0.84(2)}Y_2Ti_2O_5S_2$	$Na_{0.95(2)}Y_2Ti_2O_5S_2$	$Mg_{0.32(2)}Y_2Ti_2O_5S_2$
Ti−O2	1.7941(4)	1.8214(5)	1.8551(6)	1.8682(8)	[b]1.889(1)	1.845(1)
Ti−O1 [4]	1.9427(1)	1.9470(1)	1.9527(1)	1.9538(1)	[b]1.9526(2)	1.9588(3)
Ti−S	2.8741(6)	2.8038(7)	2.748(1)	2.740(1)	[b]2.739(2)	2.818(2)
O1−Ti−O2 [4]	104.03(1)	102.50(2)	100.78(2)	100.33(3)	[b]99.52(4)	102.61(4)
O1−Ti−O1 [4]	86.633(6)	87.315(7)	87.994(8)	88.158(9)	[b]88.43(1)	87.27(2)

[a] Values from ref 8. [b] Values obtained treating O1 as unsplit.

tropic displacement ellipsoid of the oxide ion (O1) in the TiO_2 sheets which make up the oxide slabs of the structure was extremely elongated perpendicular to the Ti−O−Ti direction and was better modeled as a site at (*x* $^1/_2$ *z*) split by reflection in the mirror plane (0 *y z*). In contrast, $Y_2Ti_2O_5S_2$[8] has O1 on the ideal (0 $^1/_2$ *z*) site with an approximately isotropic displacement ellipsoid. The analysis of $Na_{0.35(5)}Y_2Ti_2O_5S_2$ and $Na_{0.72(5)}Y_2Ti_2O_5S_2$ showed that the O1 atom in each of these phases resembled that in $Y_2Ti_2O_5S_2$ and was not significantly elongated. However, the analysis of the materials with $x > 0.7$ showed a progressive elongation of the ellipsoid. For α-$Na_{0.84(2)}Y_2Ti_2O_5S_2$ a model with O1 located at (0 $^1/_2$ *z*) and with a strongly anisotropic ellipsoid produced a comparable fit ($\chi^2 = 1.896$; $wR_p = 0.0194$) to a model with O1 treated as a split site ($\chi^2 = 1.865$; $wR_p = 0.0193$). For α-$Na_{0.95(2)}Y_2Ti_2O_5S_2$ the split site model ($\chi^2 = 2.452$; $wR_p = 0.0231$) was superior to the unsplit model ($\chi^2 = 2.678$; $wR_p = 0.0241$). Measurements carried out at 2 K for both α-$Na_{0.84(2)}Y_2Ti_2O_5S_2$ and α-$Na_{0.95(2)}Y_2Ti_2O_5S_2$ showed no gross change in structural model and suggested that α-$Na_{0.84(2)}Y_2Ti_2O_5S_2$ should be modeled using an unsplit, but elongated, O1 atom, while α-$Na_{0.95(2)}Y_2Ti_2O_5S_2$ should be modeled using a split O1 atom (although in some of what follows we use the unsplit model for this phase also). In neither the PND patterns (*d*-spacings of up to 8 Å were measured using the 35° detector bank) nor the laboratory PXRD patterns were any superstructure reflections observed; there appears, therefore, to be neither a cell expansion nor a change in space group symmetry associated with the elongation of the O1 ellipsoid. The refined atomic parameters, determined from Rietveld analysis of measurements carried out at room temperature and modeling O1 so as to give the best agreement factors for each sample, are tabulated in Table 3, and selected bond lengths and angles are shown in Table 4. The structural models obtained for a range of α-$Na_xY_2Ti_2O_5S_2$ phases are shown in Figure 2 which shows the elongation of the O1 ellipsoid as *x* approaches 1.0. Magnitudes of the diagonal elements of the U_{ij} tensor, treating O1 as unsplit, are available as Supporting Information (Figure S1).

Lithium Intercalation into α-$Na_{0.5}Y_2Ti_2O_5S_2$. Intercalation of lithium into a sample of the dark green α-$Na_{0.5}Y_2Ti_2O_5S_2$ produced a black material with a PXRD pattern showing a distribution of intensities similar to that in α-$Na_{0.5}Y_2Ti_2O_5S_2$ and consistent with $I4/mmm$ symmetry but with lattice parameters (a = 3.8905(8) Å and c = 22.242(7) Å) which were not compatible with any member of the series of intercalates α-$Na_xY_2Ti_2O_5S_2$ or $Li_xY_2Ti_2O_5S_2$.[12] Chemical analysis, after washing away the excess $LiNH_2$ formed in the reaction using dry THF, produced a composition of $Li_{0.66(5)}Na_{0.50(5)}Y_2Ti_2O_5S_2$, and Rietveld analysis of PND data in $I4/mmm$ showed that Li^+ was located in the same four-coordinate site (0 $^1/_2$ 0) as in the $Li_xY_2Ti_2O_5S_2$ series.[12] If Na^+ randomly occupies half the 12-coordinate sites in the oxide layer, and Li^+ ions are allowed to occupy all the 4-coordinate "window" sites between pairs of unoccupied 12-coordinate sites, the limiting composition matches that obtained by chemical analysis.

Magnesium Intercalation. The product of magnesium intercalation using MgH_2 was a black air-stable

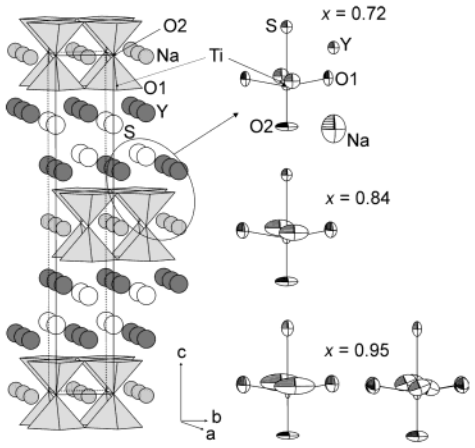

Figure 2. Structure of the α-$Na_xY_2Ti_2O_5S_2$ phases showing the intercalation of Na into the vacant sites within the oxide layers. The main part of the figure is for α-$Na_{0.72(5)}Y_2Ti_2O_5S_2$ and the detailed figures show the Ti coordination polyhedra for this phase (top) and for α-$Na_{0.84(2)}Y_2Ti_2O_5S_2$ (middle) and α-$Na_{0.95(2)}Y_2Ti_2O_5S_2$ (bottom) with anisotropic displacement ellipsoids shown at the 99% level. The elongation of the O1 ellipsoid is clearly shown, and for $x = 0.95$ this is better modeled as a split site (right bottom).

powder with tetragonal lattice parameters $a = 3.82308(4)$ Å and $c = 22.6523(3)$ Å. Rietveld analysis of PND data in space group $I4/mmm$ (Table 2) located Mg^{2+} in the 12-coordinate vacancy in the oxide blocks (i.e., the same site as is occupied by Na^+). Chemical analysis for Mg produced a composition of $Mg_{0.32(2)}Y_2Ti_2O_5S_2$, and with the composition fixed at this value in the Rietveld analysis, the refined anisotropic displacement ellipsoid was similar in dimensions to that of Na in the sodium intercalates.[19] The cell volume is consistent with the insertion of 0.64 mol of electrons per mol of $Y_2Ti_2O_5S_2$ as compared with the series of sodium and lithium intercalates. Refined atomic parameters and selected bond lengths and angles are included in Tables 3 and 4. Attempts to chemically insert additional magnesium into the host were unsuccessful.

Property Measurements. The magnetic susceptibilities of the phases α-$Na_xY_2Ti_2O_5S_2$, $Mg_{0.32(2)}Y_2Ti_2O_5S_2$, and $Li_{0.66(5)}Na_{0.50(5)}Y_2Ti_2O_5S_2$ are shown in Figure 3 as functions of temperature. The solid-state synthesis method avoids the formation of small amounts of the low-temperature ferromagnet $YTiO_3$[20] identified in our previous report of α-$Na_{1.00(2)}Y_2Ti_2O_5S_2$.[8] The curves may be fitted approximately by $\chi = \chi_0 + C/T$ and the result for α-$Na_{0.72(5)}Y_2Ti_2O_5S_2$ ($\chi_0 = 6.8(6) \times 10^{-4}$ emu mol^{-1}; $C = 0.025(1)$ emu $mol^{-1}K$) suggests that only about 20% of the inserted electrons behave as localized $S = {}^1/_2$ moments. The resistivities of the samples with $x =$ 0.35(5), 0.72(5), 0.84(2), 0.95(2), and 1.00(2) were 206, 636, 526, 95, and 95 Ωcm, respectively (with estimated errors of 10% in the measurement of these values). These values are not independent of factors such as particle size, but they indicate that the resistivities generally decrease with increasing x and the values are similar to those of lithium intercalates with similar electron counts. The values obtained for the most sodium rich materials are not inconsistent with metallic properties for these compounds. The resistivity of $Mg_{0.32(2)}Y_2Ti_2O_5S_2$ of 460 Ωcm is consistent with the values obtained for the sodium intercalates.

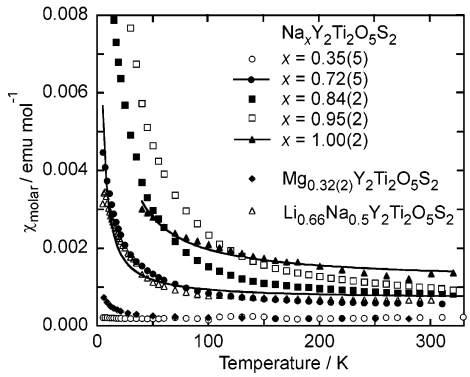

Figure 3. Magnetic susceptibilities as functions of temperature for α-$Na_xY_2Ti_2O_5S_2$ intercalates, $Mg_{0.32(2)}Y_2Ti_2O_5S_2$ and $Li_{0.66(5)}Na_{0.50(5)}Y_2Ti_2O_5S_2$. Fits to $\chi = \chi_0 + C/T$ are shown for α-$Na_{0.72(5)}Y_2Ti_2O_5S_2$ and for $Na_{1.00(2)}Y_2Ti_2O_5S_2$ above 50 K.

Discussion

The changes in structural parameters with increasing x in α-$Na_xY_2Ti_2O_5S_2$ are compared below with the changes which accompany the insertion of lithium in $Y_2Ti_2O_5S_2$.[12] When an alkali metal is inserted, the electrons enter bands which are Ti−O π-antibonding. Hence, the volume of the unit cell increases linearly with x as shown for the sodium and lithium[12] intercalates in Figure 4(c). The basal lattice parameter, a, increases linearly with x and at similar rates for the series of sodium and lithium intercalates, α-$Na_xY_2Ti_2O_5S_2$ and $Li_xY_2Ti_2O_5S_2$ (Figure 4(a)). The lattice parameter c, perpendicular to the layers, decreases monotonically with x in the lithium intercalates, but in the case of sodium intercalation reaches a minimum at around $x = 0.7$, and then increases with x (Figure 4(b)). The increase in the c lattice parameter for $0.7 < x < 1.0$ is found to coincide with the pronounced elongation of the O1 ellipsoid.

As electrons are added to Ti−O antibonding crystal orbitals the Ti−O distances all increase as shown in Figure 5. The O2−Ti−O1 angle (Figure 5(c)) decreases linearly with increasing x, and the coordination around Ti tends toward a regular octahedron with a sharply decreasing Ti−S distance (Figure 6). This change in Ti environment is partly driven by electronic considerations (the loss of Ti−O bonding is minimized, and the Ti−S bonding is enhanced) as described for the lithium intercalates in ref 12. The coordination of Ti by oxide varies in a very similar way with x in both $Li_xY_2Ti_2O_5S_2$ and α-$Na_xY_2Ti_2O_5S_2$. The trends in Ti−O2, Ti−O1 distances and O1−Ti−O2 and O1−Ti−O1 angles for the two series of compounds follow one another very closely over the range $0 < x < 1.0$ as shown in Figure 5. For $x < 0.7$, the Ti−S distance in α-$Na_xY_2Ti_2O_5S_2$ also follows the trend shown by $Li_xY_2Ti_2O_5S_2$ (Figure 6). However, in the range $0.7 < x < 1.0$, the behaviors of the sodium intercalates and the lithium intercalates are different. In the lithium intercalates[12] the Ti−S distance decreases linearly with x reaching a minimum value of 2.512(5) Å in $Li_{1.85}Y_2Ti_2O_5S_2$[12] compared with the value

(19) A freely refined Mg occupancy produced a composition of $Mg_{0.19(1)}Y_2Ti_2O_5S_2$, but with a displacement ellipsoid a factor of 10 smaller than that for the same site in the sodium intercalates.

(20) Greedan, J. E. *J. Less Common Met.* **1985**, *111*, 335.

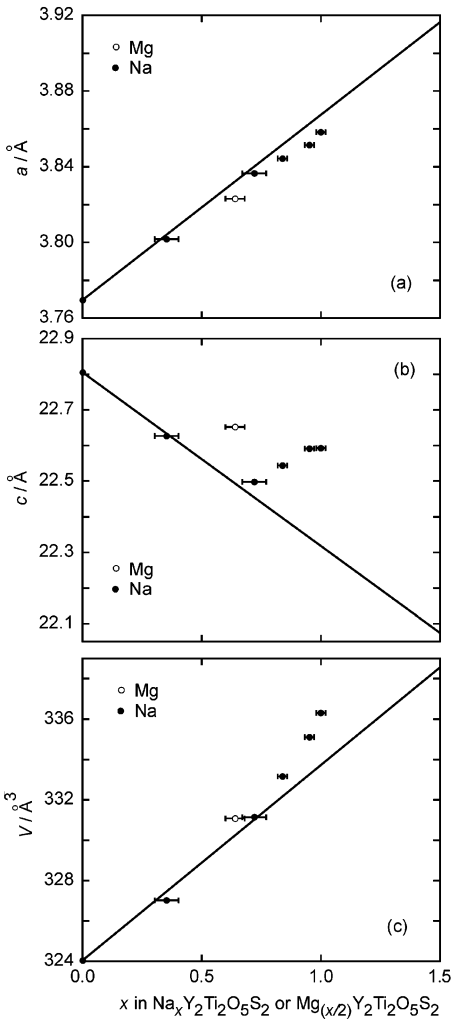

Figure 4. Lattice parameters and unit cell volume for α-$Na_xY_2Ti_2O_5S_2$ ($0 < x \leq 1$) as functions of x: (a) basal lattice parameter a; (b) lattice parameter c; and (c) volume. The lines show, for comparison, the approximately linear mean trends in these parameters for the analogous lithium intercalates $Li_xY_2Ti_2O_5S_2$ ($0 < x \leq 2$).[12] Data for $Mg_{0.32(2)}Y_2Ti_2O_5S_2$ are also shown for comparison.

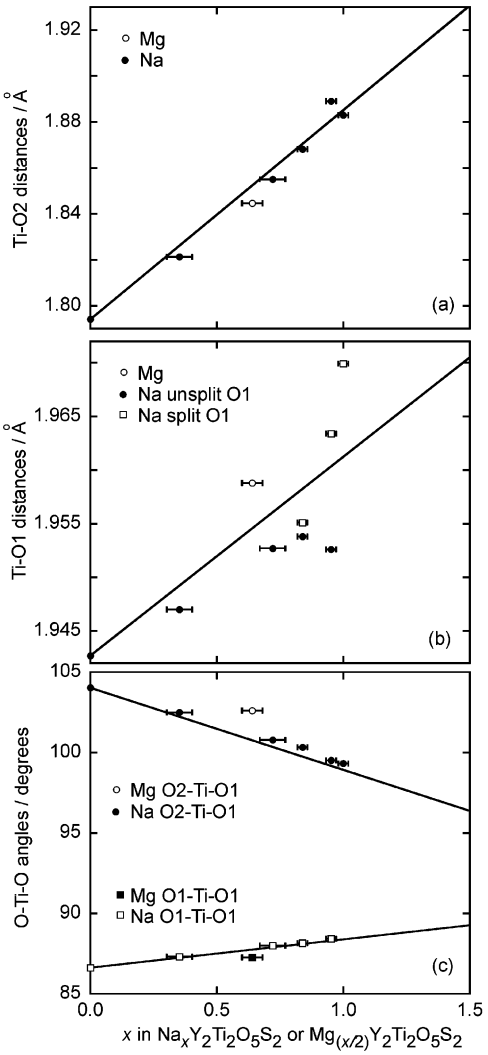

Figure 5. Axial Ti−O2 bond lengths (a); the equatorial Ti−O1 bond lengths (b); and the O2−Ti−O1 and O1−Ti−O1 bond angles (c) as functions of x for α-$Na_xY_2Ti_2O_5S_2$. The lines show, for comparison, the approximately linear mean trends in these parameters for the analogous lithium intercalates $Li_xY_2Ti_2O_5S_2$.[12] Data for $Mg_{0.32(2)}Y_2Ti_2O_5S_2$ are also shown for comparison.

of 2.8741(6) Å in $Y_2Ti_2O_5S_2$.[8] Inspection of the Ti−S distances for α-$Na_xY_2Ti_2O_5S_2$ shows that they approach a limiting value of 2.732(3) Å in α-$Na_{1.00(2)}Y_2Ti_2O_5S_2$,[8] compared with 2.6791(8) Å in the "isoelectronic" $Li_{0.99(5)}Y_2Ti_2O_5S_2$.[12] The changes in the titanium environment are not independent of the requirements of the yttrium ion and the intercalated alkali metal cation. The Y−Na distances in α-$Na_xY_2Ti_2O_5S_2$ (Figure 7(a)) should be compared with the corresponding distance in $Li_xY_2Ti_2O_5S_2$ which is between Y and the center of the 12-coordinate vacancy ($^{12}\square$) in the oxide slabs. This site remains unoccupied in the lithium intercalates because lithium occupies a site completely different from that occupied by sodium. The Y−$^{12}\square$ distance decreases monotonically over the full range of Li intercalation (Figure 7(a)) showing that there is no impediment to shortening of this separation. The corresponding Y−Na distance in the sodium intercalates decreases in the range $0 < x < 0.7$, reaching a minimum value of about 3.74 Å, and then increases (Figure 7(a)). This is presumably a consequence of electrostatic repulsion between Y^{3+} and Na^+,[21] which does not occur in the

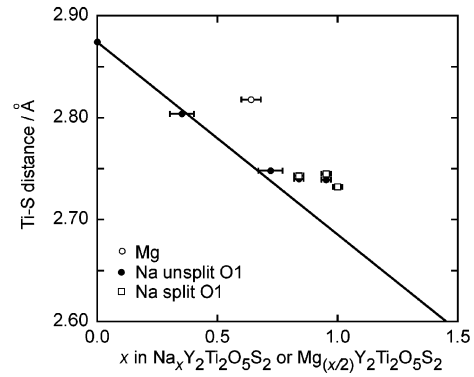

Figure 6. Axial Ti−S distance as a function of x for intercalates α-$Na_xY_2Ti_2O_5S_2$. The line shows, for comparison, the linear mean trend in the Ti−S distance for the analogous lithium intercalates $Li_xY_2Ti_2O_5S_2$.[12] Data for $Mg_{0.32(2)}Y_2Ti_2O_5S_2$ are also shown for comparison.

lithium intercalates. The effect of this is that the mean Y−O1 distances (Figure 7(b)) increase much more in the sodium intercalates than in the lithium intercalates,

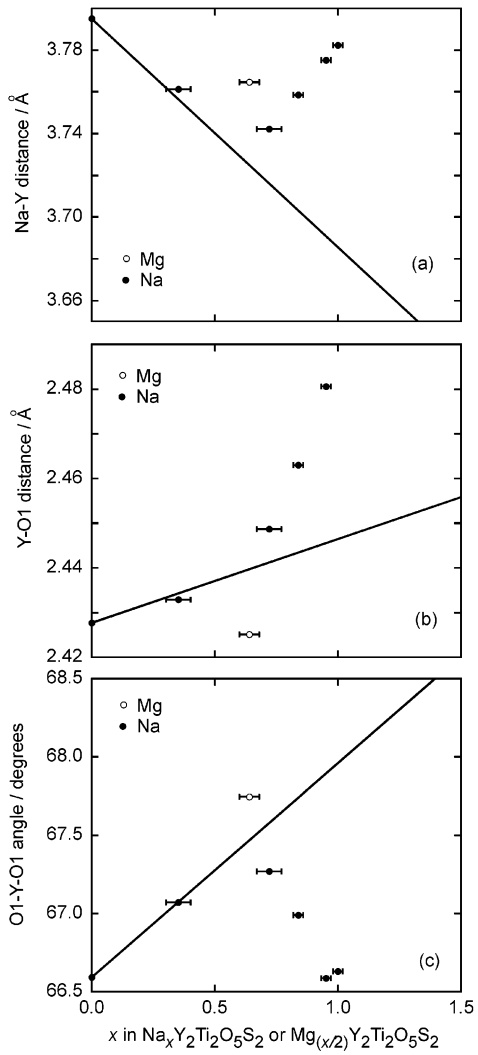

Figure 7. (a) Na−Y distance as a function of x for intercalates α-$Na_xY_2Ti_2O_5S_2$ compared with the distance between Y and the center of the empty 12-coordinate site in the analogous lithium intercalates $Li_xY_2Ti_2O_5S_2$[12] (line). (b) The Y−O1 distances and (c) the O1−Y−O1 angles in α-$Na_xY_2Ti_2O_5S_2$ compared with the approximately linear mean trends (lines) in these parameters for $Li_xY_2Ti_2O_5S_2$.[12] Data for $Mg_{0.32(2)}Y_2Ti_2O_5S_2$ are shown for comparison.

and the O1−Y−O1 angles (Figure 7(c)) reach a maximum for $x = 0.7$, and then decrease, reaching a value in α-$Na_{1.00(2)}Y_2Ti_2O_5S_2$[8] similar to that in $Y_2Ti_2O_5S_2$. The Ti−S distance, which shortens to a Ti−S bonding distance in the lithium-rich intercalates,[12] is not independent of the coordination around yttrium, so the effect of Na^+-Y^{3+} repulsion is to curtail the decrease in Ti−S distance, and also to increase the length of the c axis in the range $0.7 < x < 1.0$ in α-$Na_xY_2Ti_2O_5S_2$ in contrast with the monotonic decrease of c with x in the range $0 < x < 2$ in the lithium intercalates.[12] Comparison of the behavior of the single magnesium intercalate investigated suggests that while the increase in cell volume with electron count is independent of the intercalant (Figure 4(c)), the charge on the intercalant ion, as well as its location, is important in determining precise bond lengths and angles (Figures 5, 6, and 7).

In the $Li_xY_2Ti_2O_5S_2$ series[12] there is a structural distortion in the approximate composition range $0.7 < x < 1.3$ which is electronically driven, and is of the cooperative Jahn−Teller type. This distortion can be rationalized using extended Hückel type calculations,[12] and the effect is to lower the site symmetry of the titanium ion from 4*mm* to *mm*2, and the space group symmetry from tetragonal *I*4/*mmm* to orthorhombic *Immm*. The Li^+ ion occupies a site of *mmm* symmetry in the *I*4/*mmm* space group and orders between two inequivalent sites also with *mmm* symmetry in the *Immm* space group. The distortion minimizes the loss of Ti−O bonding incurred on occupation of crystal orbitals which are formally antibonding.[12] Although the changes in geometry at the Ti centers in the $Li_xY_2Ti_2O_5S_2$ and α-$Na_xY_2Ti_2O_5S_2$ intercalates are similar, the sodium intercalates do not show the cooperative structural distortion observed in the lithium intercalates. Location of Na^+ in the 12-coordinate site of 4/*mmm* symmetry, rather than in the 4-coordinate site of *mmm* symmetry occupied by Li^+ in $Li_xY_2Ti_2O_5S_2$, removes the cooperative distortion coordinate (i.e., distortion would lower the symmetry of the alkali cation). The occurrence of the elongated/disordered O1 atom in the α-$Na_xY_2Ti_2O_5S_2$ intercalates occurs in the range of values of x for which the lithium intercalates distort to orthorhombic symmetry. This subtle change in the structural model for the α-$Na_xY_2Ti_2O_5S_2$ intercalates could therefore be interpreted as also being electronic in origin, but prevented from occurring cooperatively by the different location of the alkali cation. An alternative interpretation of the behavior of the O1 ellipsoid is that it indicates tilting of the TiO_5S polyhedra relative to one another in response to the coordination requirements of the Na^+ cation in a manner similar to the distortions which control the detailed structures of perovskite and perovskite-related phases.[22] The lack of superstructure reflections and the modeling of O1 as an elongated or split site are consistent with this, providing that the sense of the tilting is not periodic in the direction perpendicular to the layers.

The measurements of electrical resistivities of the sodium and magnesium intercalates are consistent with those of the analogous lithium intercalates showing, despite the difficulties in making measurements of absolute values, a general decrease in resistivity with increasing electron count. The value for α-$Na_{0.95(2)}Y_2Ti_2O_5S_2$ of 95(9) Ωcm is similar to that for the isoelectronic lithium intercalate $Li_{0.99(5)}Y_2Ti_2O_5S_2$ (50(5) Ωcm).[12] These values are not inconsistent with metallic conductivity at the highest values of x, and the delocalization of electrons is supported by the large temperature-independent contribution and the small Curie contribution to the magnetic susceptibilities. In contrast, the intercalates β-$NaY_2Ti_2O_5S_2$ and $KY_2Ti_2O_5S_2$ with the alkali metal in the sulfide layer[8,14] have resistivities 2−4 orders of magnitude larger (β-$NaY_2Ti_2O_5S_2$, $1.5(5) \times 10^5$ Ωcm; $KY_2Ti_2O_5S_2$, $4.4(5) \times 10^4$ Ωcm)[14] than those of the isoelectronic $Li_xY_2Ti_2O_5S_2$ and α-$Na_xY_2Ti_2O_5S_2$ intercalates.

In summary, the $Ln_2Ti_2O_5S_2$ systems[9,10] are not only of interest for their properties as narrow band gap

(21) O'Keeffe, M.; Hyde, B. G. In *Structure and Bonding in Crystals Vol. 1*; O'Keeffe, M., Navrotsky, A., Eds.; Academic Press: New York, 1981.

(22) Glazer, A. M. *Acta Crystallogr.* **1972**, *B28*, 3384.

semiconductors,[23,24] but their wide range of alkali and alkaline earth metal intercalates[11,12,14] has opened up novel possibilities with respect to intercalation on Ruddlesden−Popper phases, and also provides systems in which the effects of electron count on structures and properties in two dimensions may be probed.

Acknowledgment. We thank the U.K. EPSRC (grant GR/N18758) for funding and access to ISIS and ILL. S.J.C. thanks the Royal Society for further financial support. We are grateful to Dr. R. I. Smith (ISIS Facility) for assistance with measurements carried out at ISIS.

Supporting Information Available: Table of magnitudes of the diagonal elements of the U_{ij} tensor, treating O1 as unsplit (pdf). This material is available free of charge via the Internet at http://pubs.acs.org.

CM034762F

(23) Boyer-Candalen, C.; Derouet, J.; Porcher, P.; Moëlo, Y.; Meerschaut, A. J. *Solid State Chem.* **2002**, 165, 228.

(24) Ishikawa, A.; Takata, T.; Kondo, J. N.; Hara, M.; Kobayashi, H.; Domen, K. *J. Am. Chem. Soc.* **2002**, 124, 13551.